A scenic view of a body of water, likely the Japan/East Sea, with trees in the foreground and a sailboat in the distance. The text is overlaid on the water.

**Low frequency
variability of sea level in
the Japan/East Sea,
estimated from AVISO
satellite altimetry**

O. Trusenkova and D. Kaplunenko
Pacific Oceanological Institute, Vladivostok, Russia
PICES-2010, October 22-31, 2010, USA, Portland

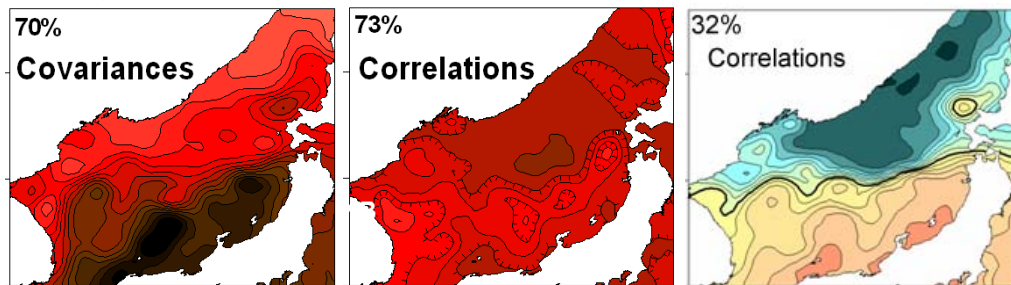
Motivation:

the previous analysis of the seasonal SLA in the JES
from $1/3^\circ$ -gridded reference AVISO product

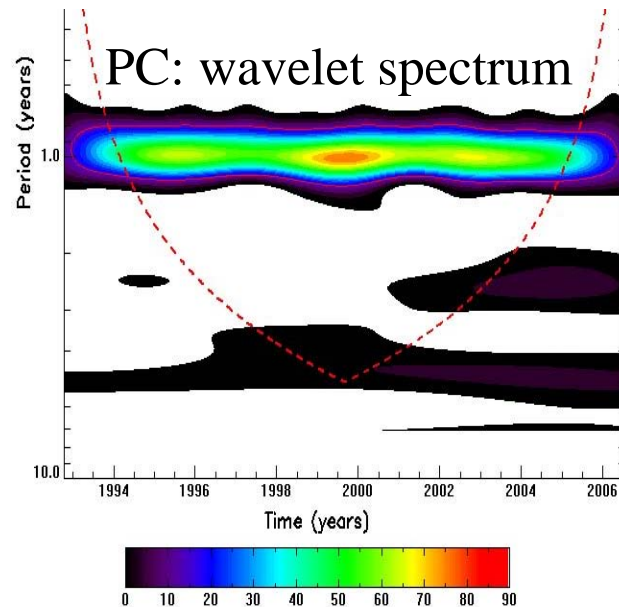
Interacting modes derived from
the successive EOF decompositions

Synchronous Mode

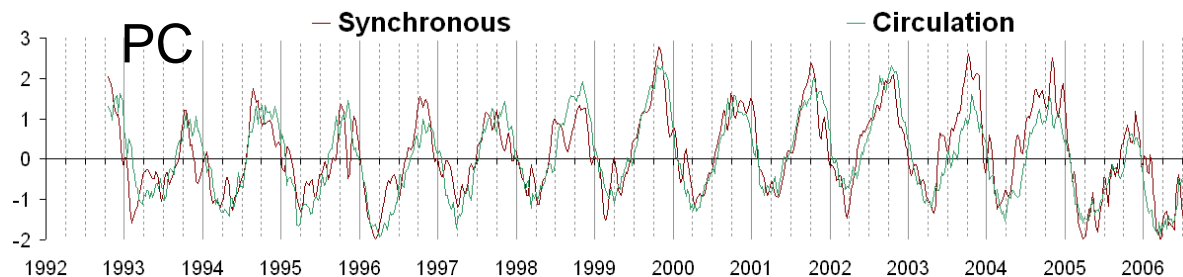
Circulation Mode



Decomposition 1a Decomposition 1b Decomposition 2



Power on the annual
time scale only



The strong seasonal signal suppresses interannual variability

Purpose

To reveal interannual variability of sea level in the JES using low-pass filtered AIVSO altimetric $1/4^\circ$ -gridded SLA.

To compare EOF patterns from reference and update products.

Data

AVISO weekly reference and update $1/4^\circ$ -gridded SLA, October 1992 - October 2009, 891 times total, 35.5° - 48° N, 127.5° - 142° E.

Reference data from 2 satellites for the whole period.

Update data from all available satellites (3-4 at some times) → comparison between times may be biased.

Errors were previously estimated as 4-4.5 and 3.5-4 cm in the southern and northern JES, respectively.

Decomposition to EOF implies averaging, therefore errors are decreased by \sqrt{N} (Preisendorfer, 1988); $N = 891$.

Errors of SLA contributions from EOF modes are decreased by ~ 0.035 .

Techniques of EOF analysis

Traditional EOF analysis: a set of orthogonal patterns focused on areas of large variance.

1) Covariances \sim signal magnitude \rightarrow anomalies from weaker signals can be lost.

Correlations (normalized fields) \rightarrow detection of small amplitude anomalies, such as SLA in the northern JES

2) Natural patterns are not necessarily orthogonal. However, orthogonality is intrinsic to EOF patterns and larger gap between the eigenvalues, stronger constraint on higher modes.

Successive decompositions after the removal of contribution of a leading mode.

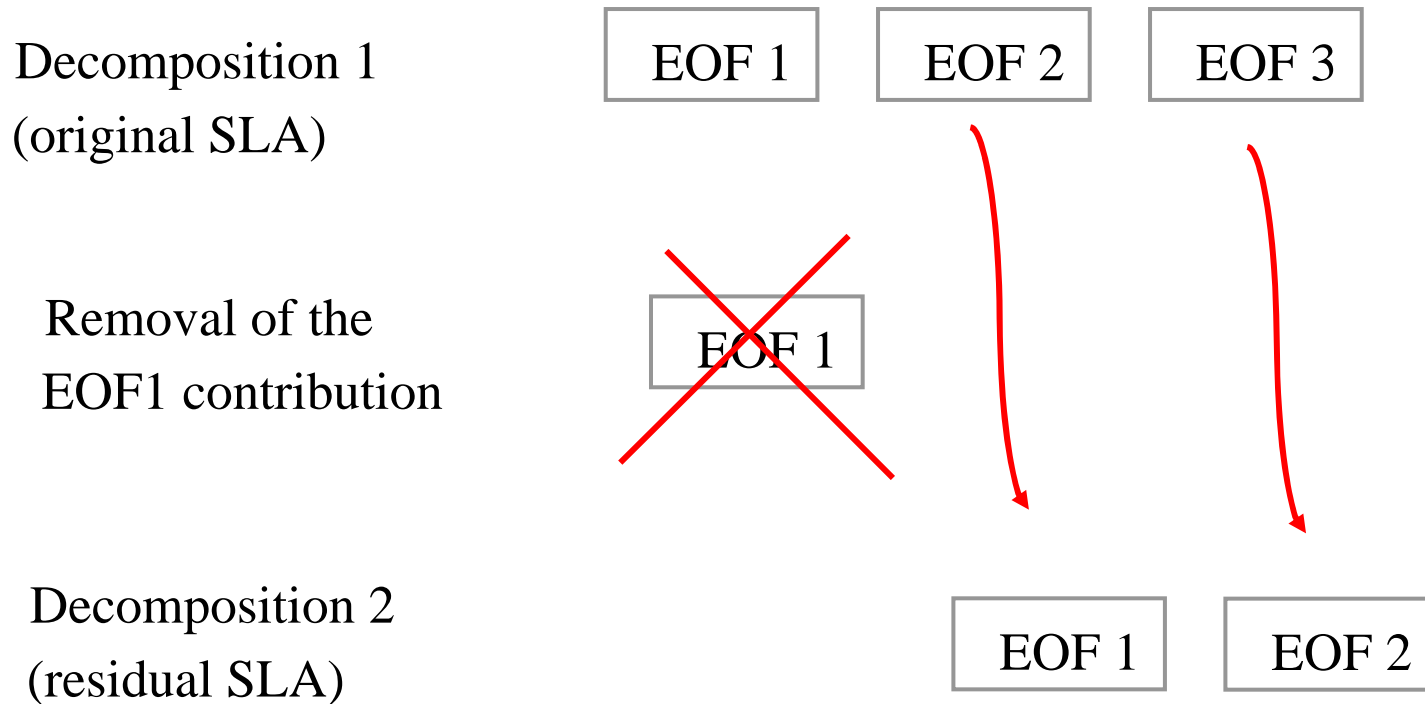
Residual anomalies: $\zeta_2(\mathbf{r}, t) = \zeta_1(\mathbf{r}, t) - A_1(\mathbf{r}) \cdot B_1(t) \rightarrow$

pre-normalization provided by correlations allows for pattern adjustment in the second decomposition, while covariance-based patterns would not change.

This approach was applied to SST (Trusenkova et al., 2009) and SLA

(presented at PICES 2009).

Successive decompositions: orthogonal modes

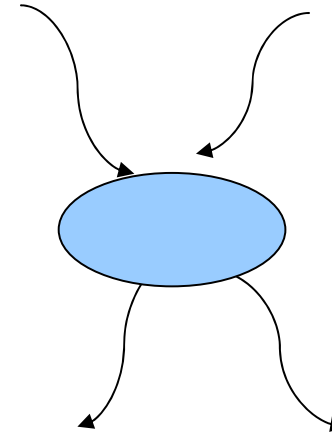


Successive decompositions: non-orthogonal modes

Decomposition 1
(original SLA)



Removal of the
EOF1 contribution



Decomposition 2
(residual SLA)



Successive decompositions: breaking up modes

Decomposition 1
(original SLA)

EOF 1

EOF 2

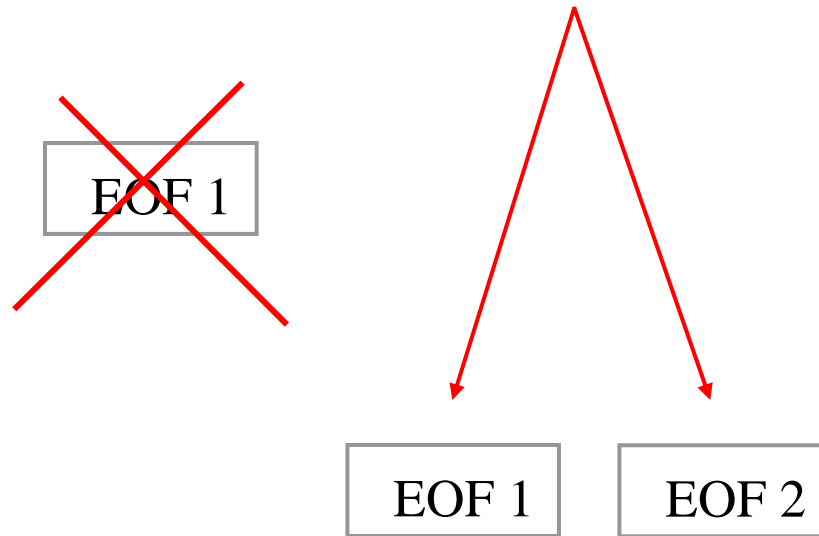
Removal of the
EOF1 contribution

~~EOF 1~~

Decomposition 2
(residual SLA)

EOF 1

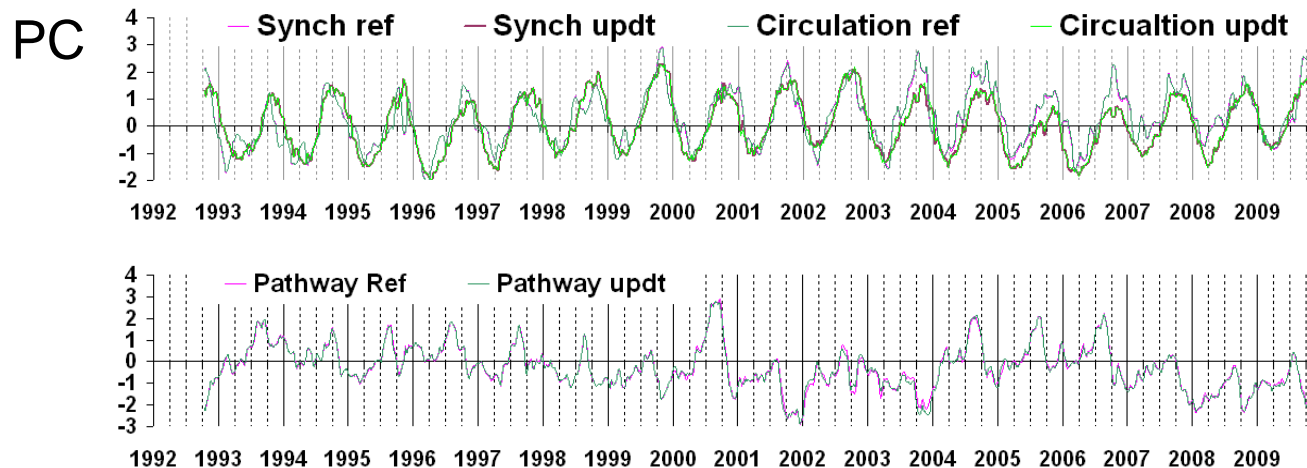
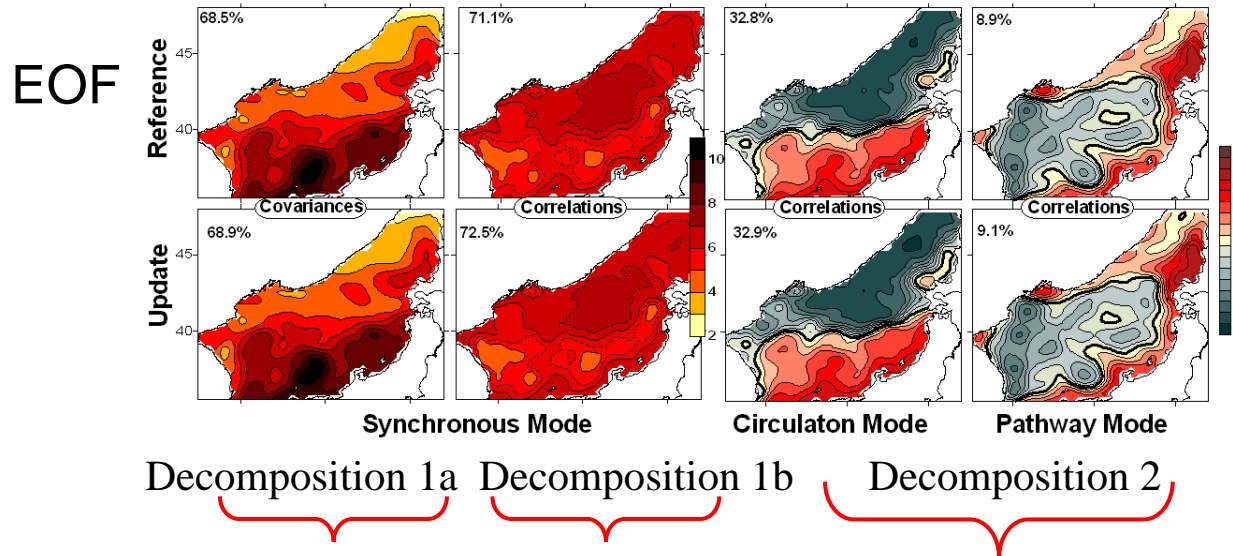
EOF 2



EOF analysis

- covariance-based decomposition 1a of the original reference and update SLA;
- correlation-based decomposition 1b of the original reference and update SLA;
- removal the contribution of the correlation-based leading mode;
- correlation-based decomposition 2 of the residual reference and update SLA.

Seasonal signals from the reference and update data

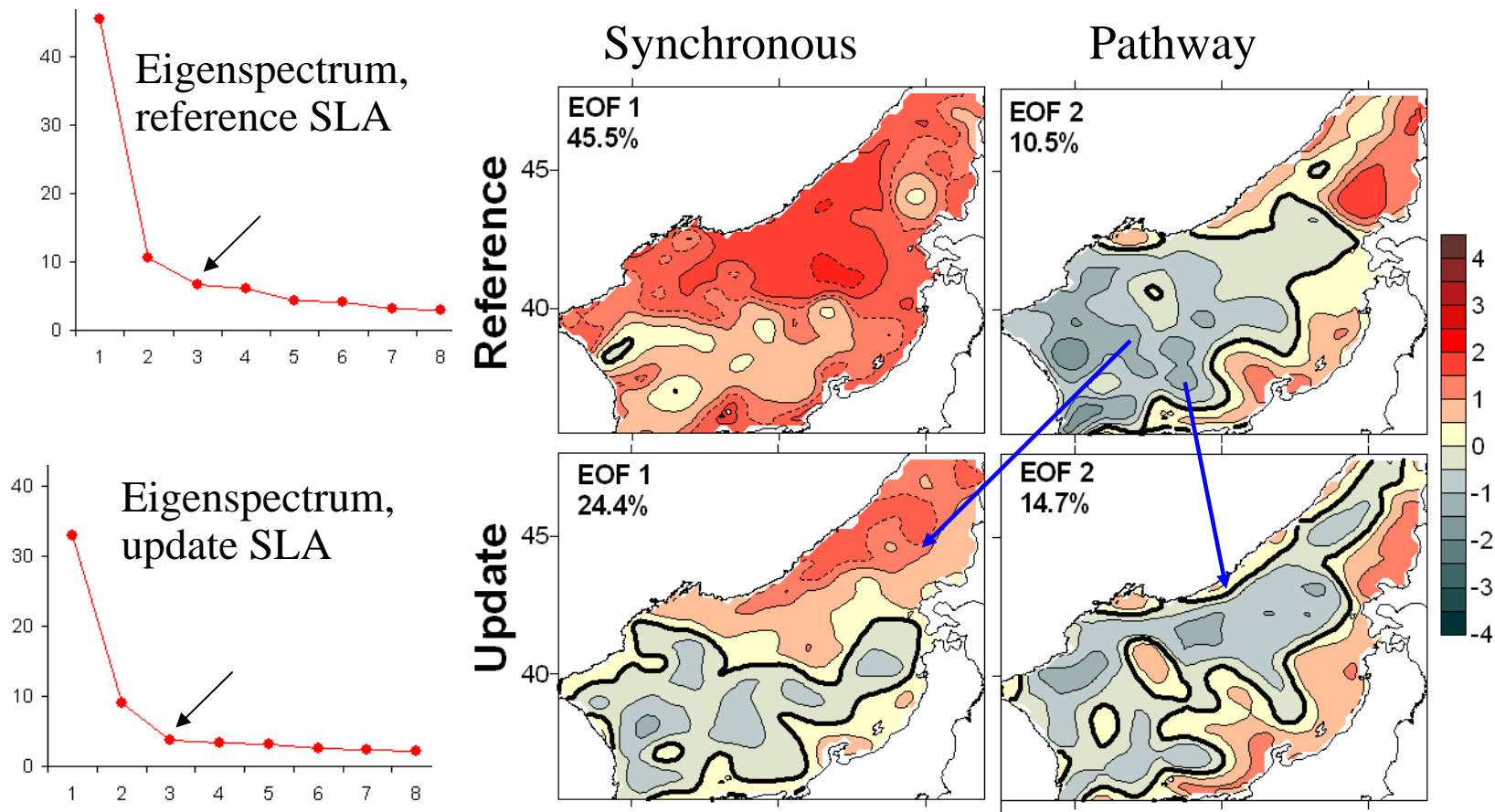


Patterns are the same

Data processing

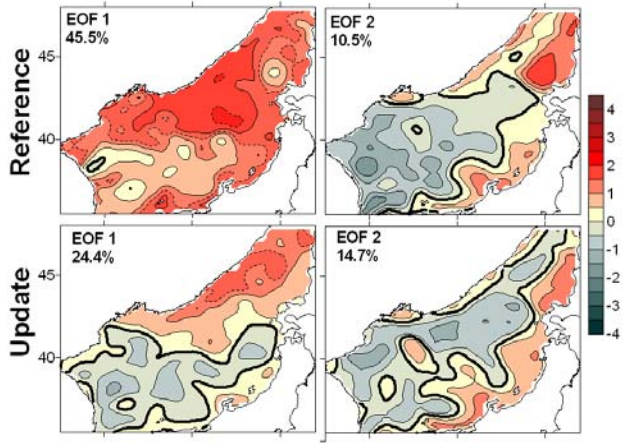
Low-pass filtering by wavelet transform using Morlet mother wavelet, with the cut-off period of 1.2 year.
EOF decompositions of the low-pass filtered reference and update LSA, using both correlations and covariances

Correlation-based decompositions of the low frequency reference and update SLA

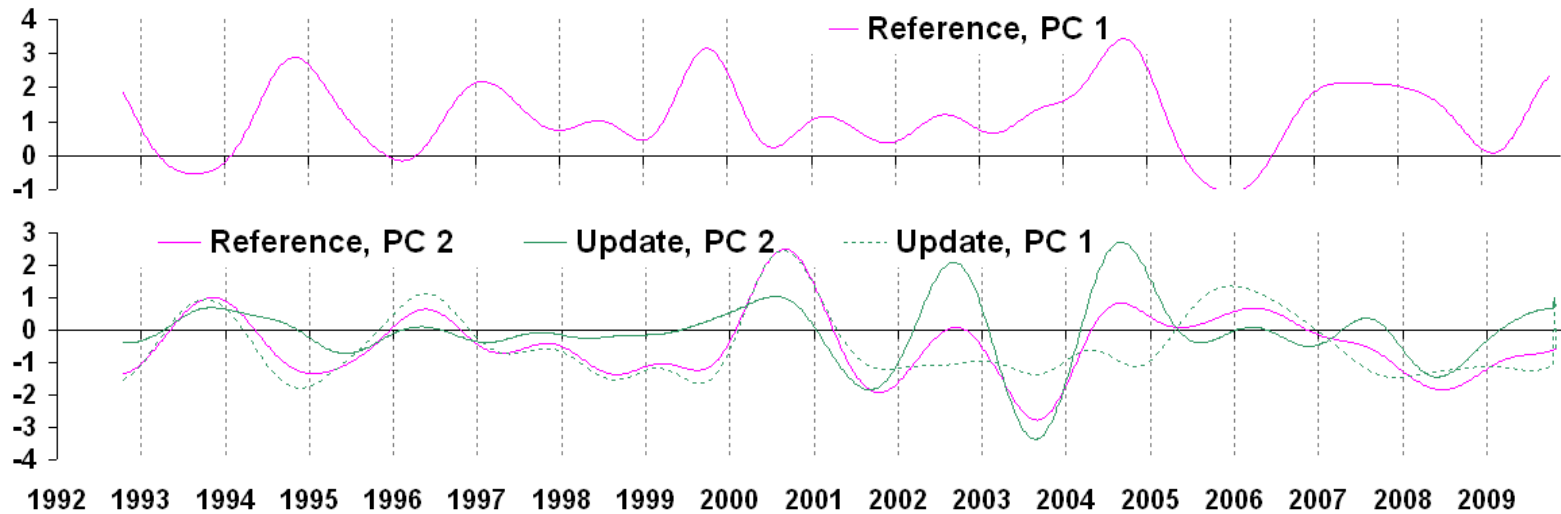


Statistically significant modes 1 and 2 from both decompositions.

No analog of the synchronous reference mode 1 in the update SLA;
the reference mode 2 breaks up to the update modes 1 and 2.



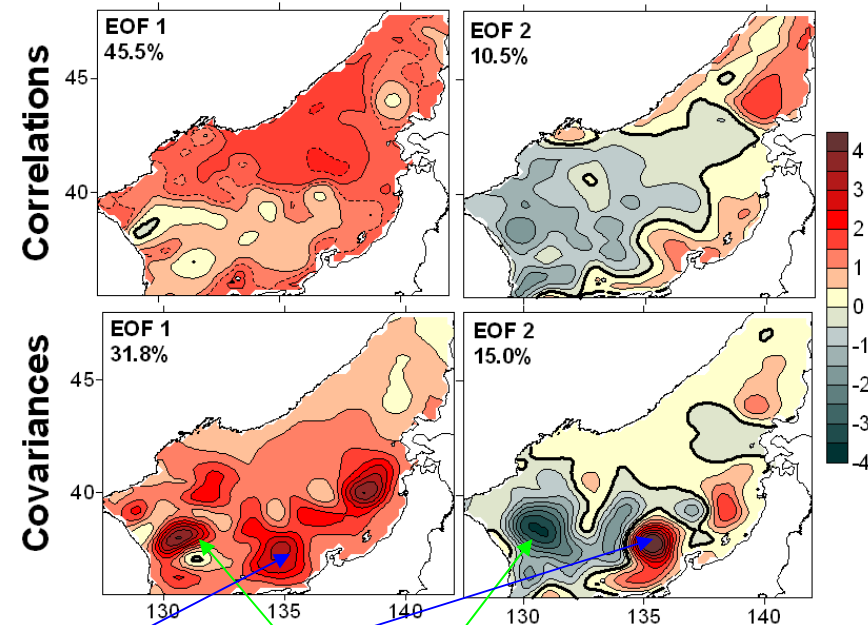
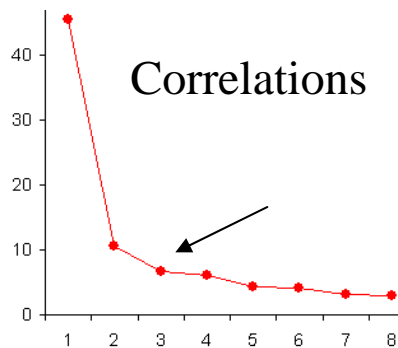
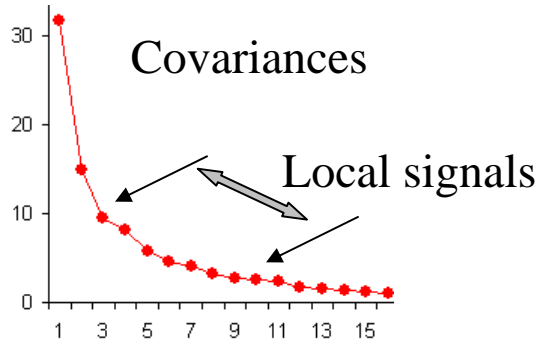
Temporal patterns are similar in some periods, different in other times → spurious signals in the update SLA due to the changing data coverage?



Reference SLA: correlations vs. covariances

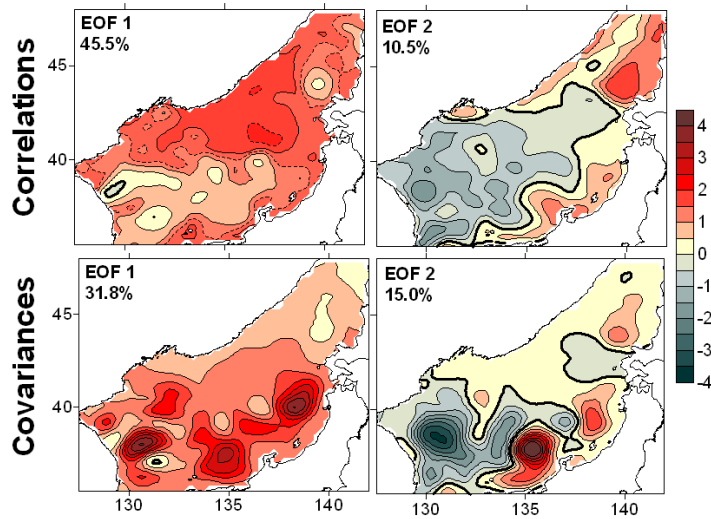
Covariance modes 3+:
contributions from mesoscale processes

Eigenspectrums



Large loadings in the areas of frequent eddies: Ulleung Warm Eddy, the meandering TWC off Honshu

Seesaw between the SW and SE JES (Morimoto and Yanaigi, 2001; Choi et al., 2004).
Covariance modes similar to those by Choi et al. (2004).

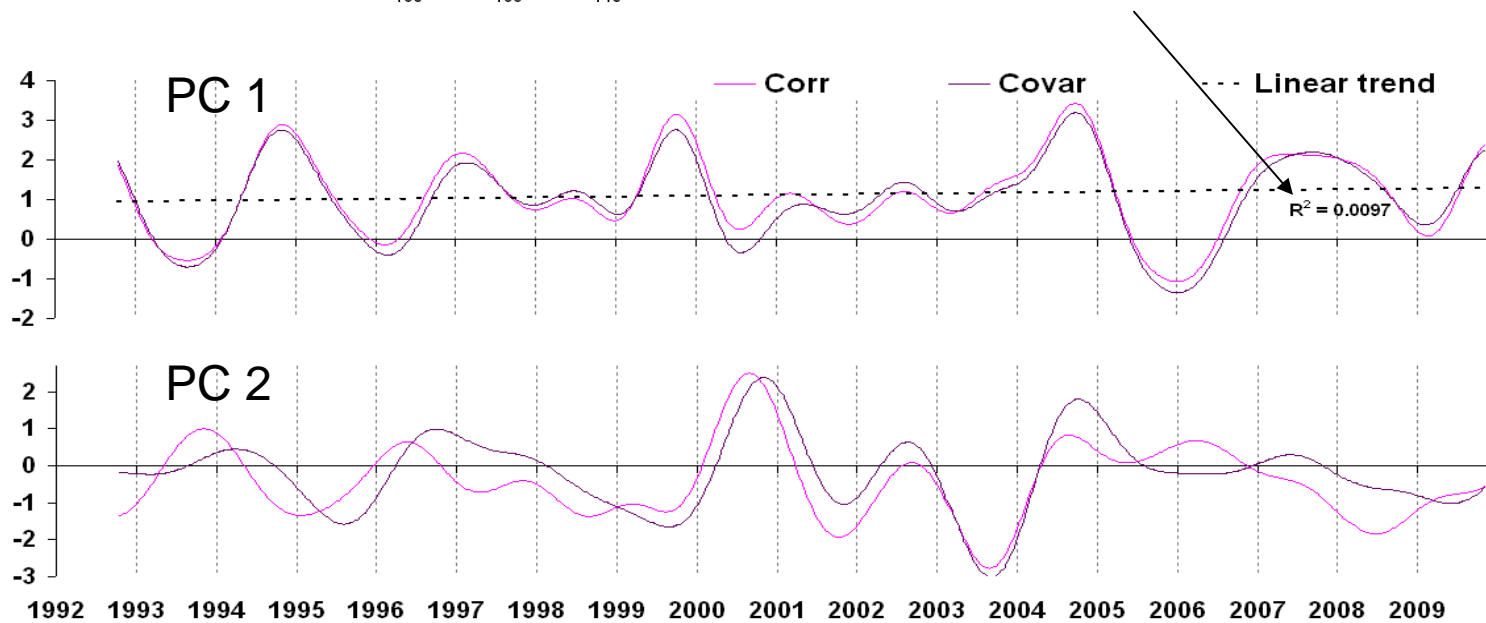


Similar temporal patterns:

$$R_{PC1} = 0.976$$

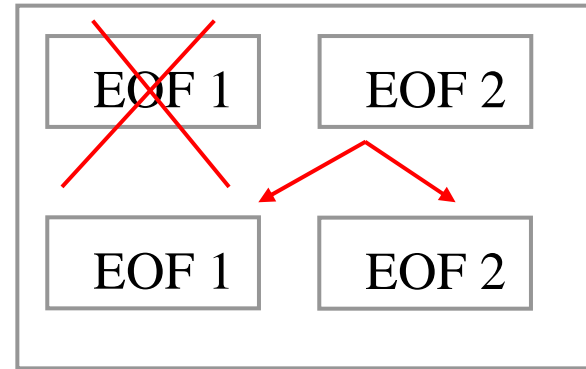
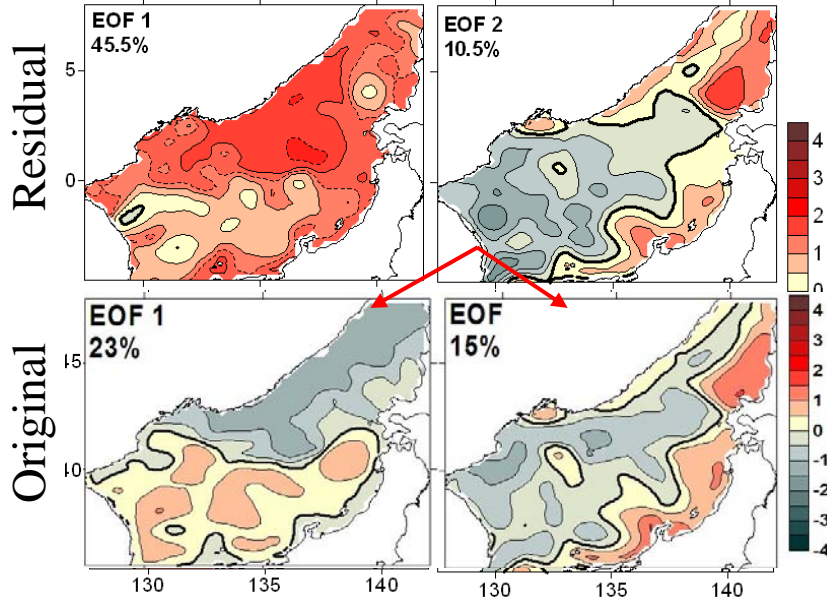
$$R_{PC2} = 0.771$$

No statistically significant trend

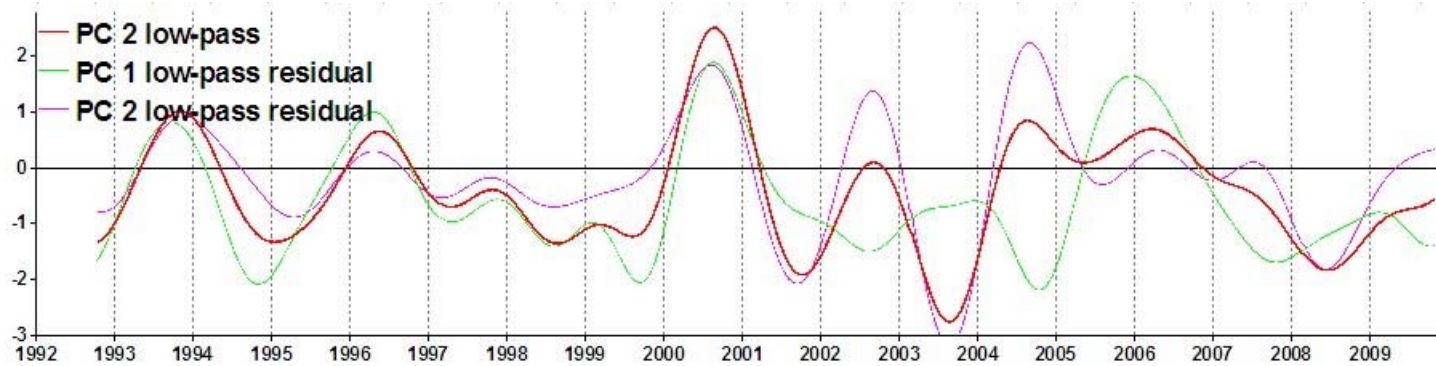


Comparison of the original and residual modes

Decomposition 1 Decomposition 2

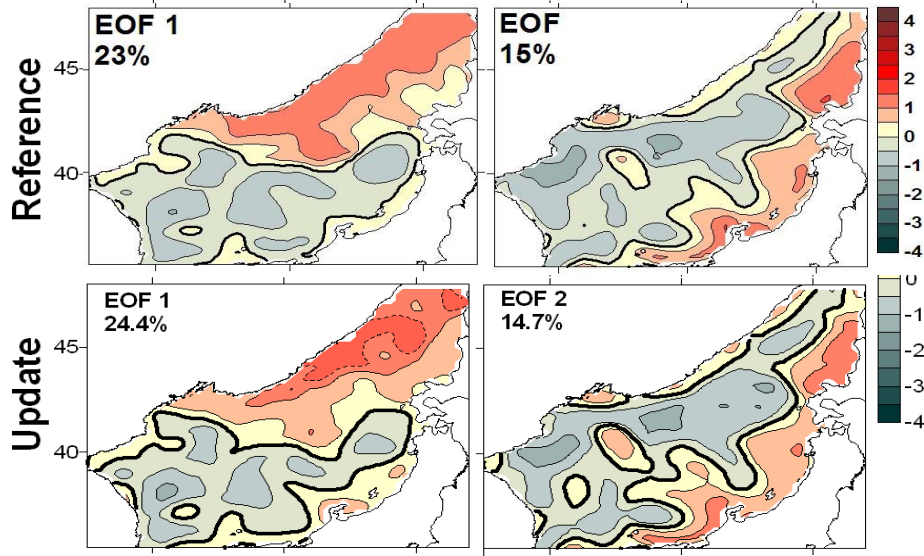


Mode 2 breaks up,
similar to the update mode.

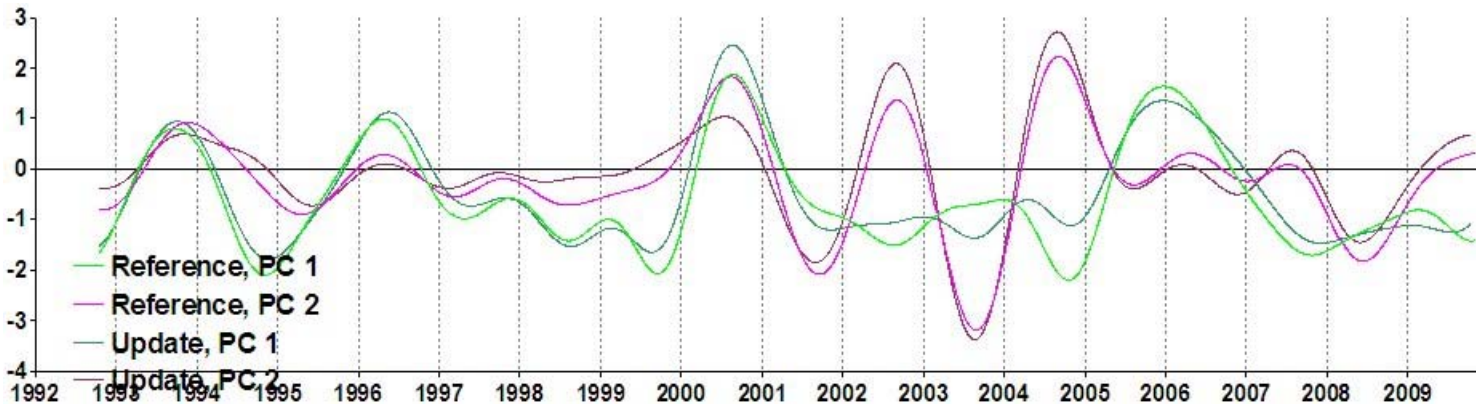


EOF modes from residual low frequency reference SLA (Decomposition 2)

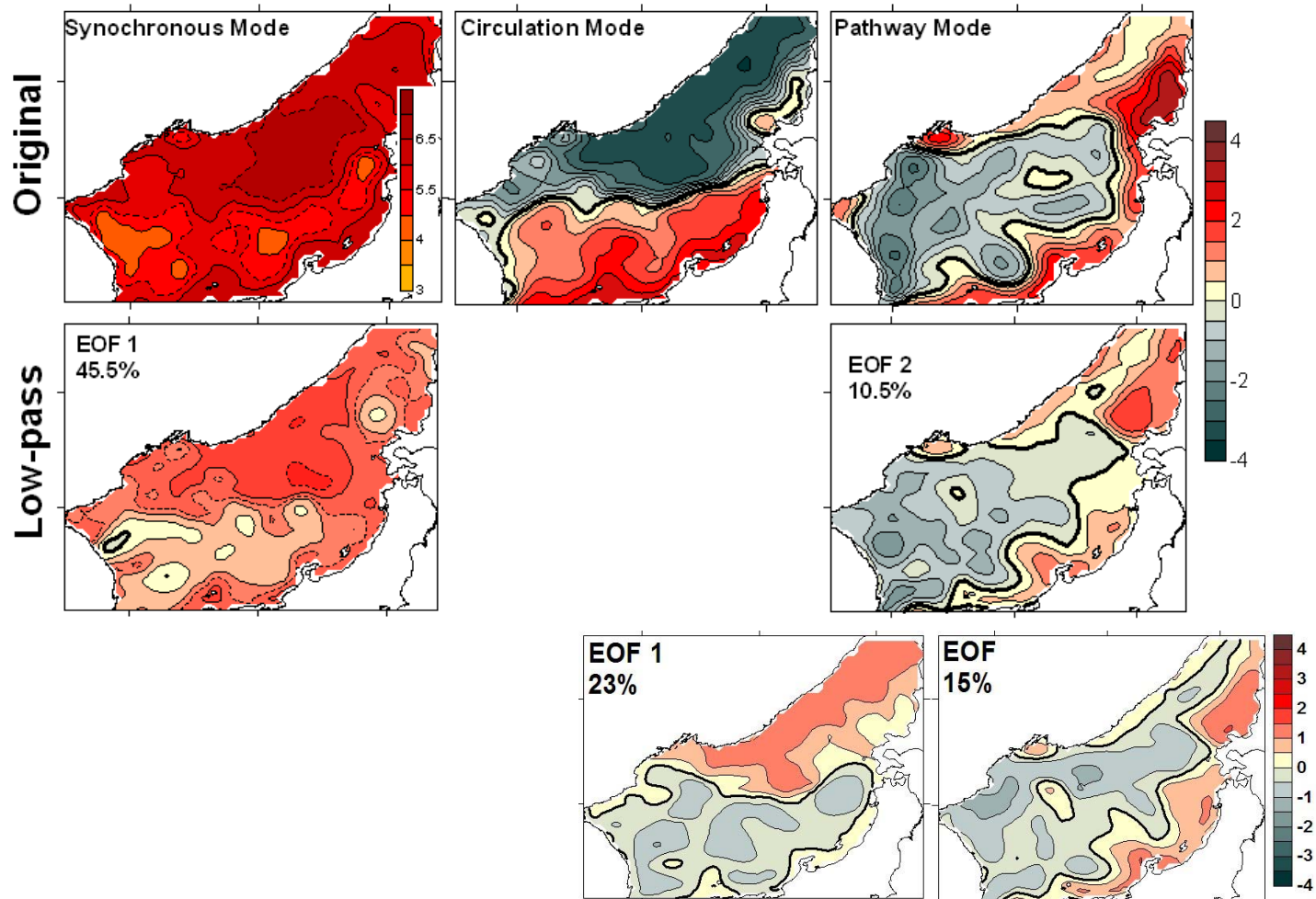
Decomposition 1b Decomposition 2



Patterns from the residual reference SLA are similar to the interannual update patterns.



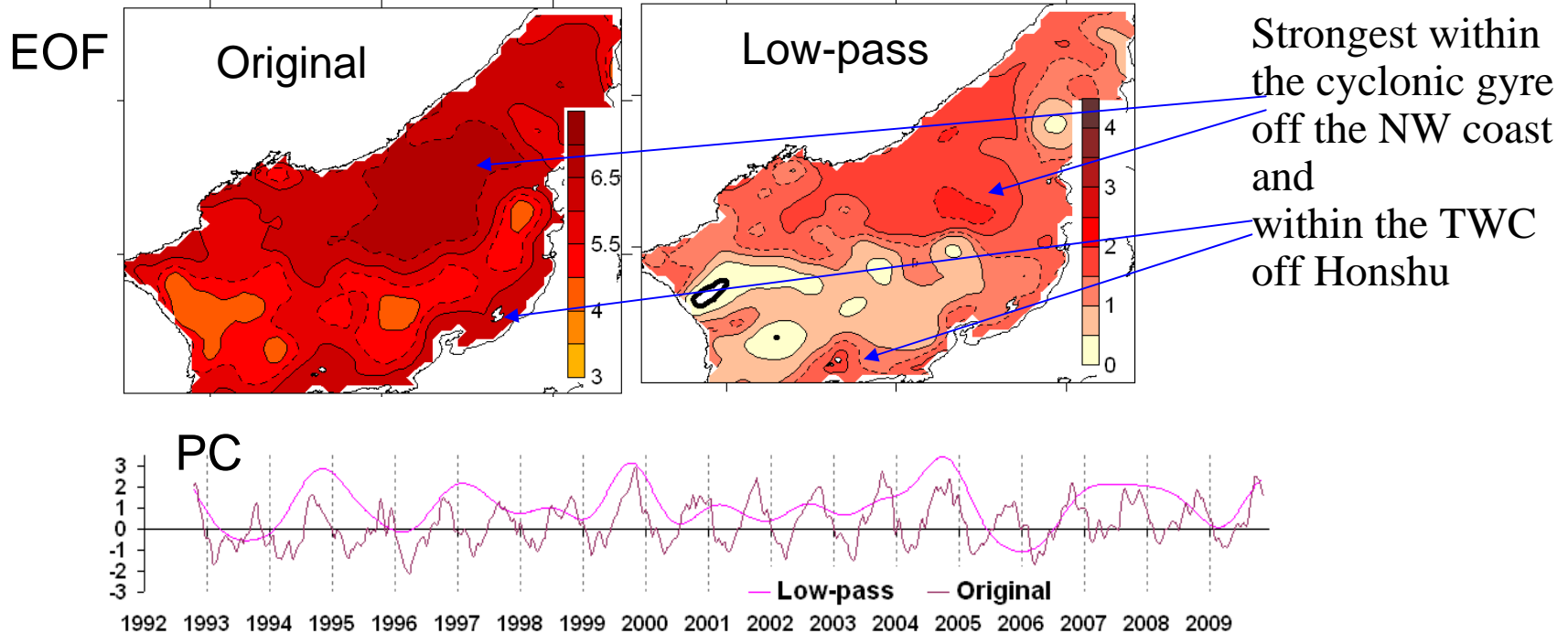
Intercomparison of the original and low frequency reference modes



No low-frequency counterpart of the seasonal Circulation Mode.

Interannual Synchronous Mode

Similar spatial patterns



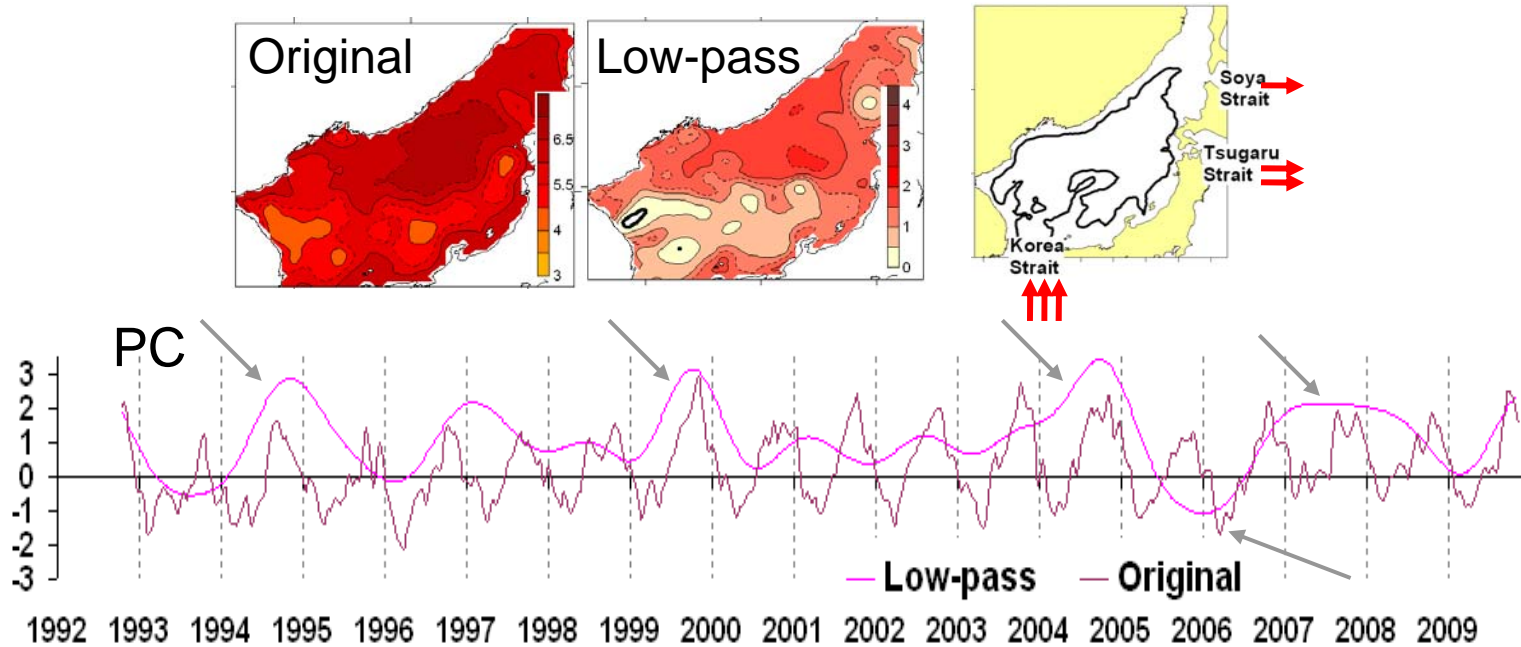
SLA related to the low frequency mode are weak (0.5-3 cm) but exceed errors of the gridded SLA, considering the averaging intrinsic to EOF decomposition:
 $ERR_{orig}/\sqrt{N} = (4.5)/29.8 \sim 0.15 \text{ cm}.$

Average SLA above the data errors but should be zero!

Period for mean sea level: 1993-1999, SLA for the 1992-2009.

What happened afterwards?

Quasi-biennial Synchronous Mode



Suggested forcing

- of the seasonal Synchronous Mode: steric signal and volume imbalance,
- of the interannual Synchronous Mode: volume imbalance.

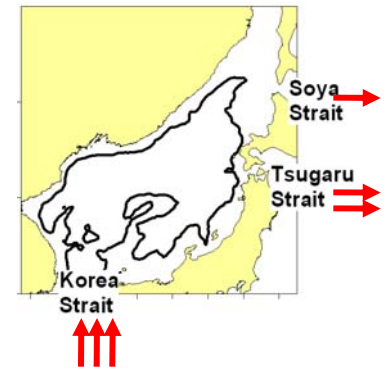
SLA of 0.5-3 cm correspond to .4-2% of volume imbalance.

Considerable sea level rise in 1994, 1999, 2004, 2007-2008 and decline from July 2005 through June 2006.

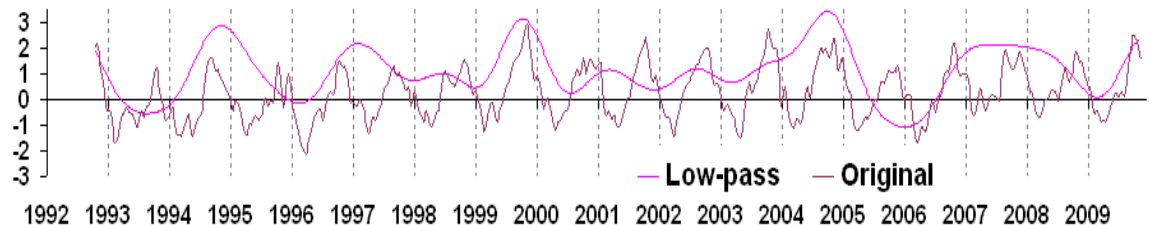
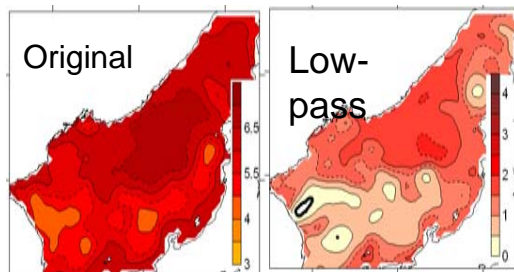
Transport in the Korea Strait has been largest (smallest) in 1999 (2005) since 1997 (ferry-mounted ADCP; Ostrovskii et al., 2009).

Quasi-biennial variation

Large-scale and local differences of sea level and wind stress curl, propagation of coastal trapped waves as forcings of transport through the straits (Lyu and Kim, 2005; Tsujino et al., 2008; Mon et al., 2009) and of the through-flow transport from cable voltage (Palshin et al., 2001).

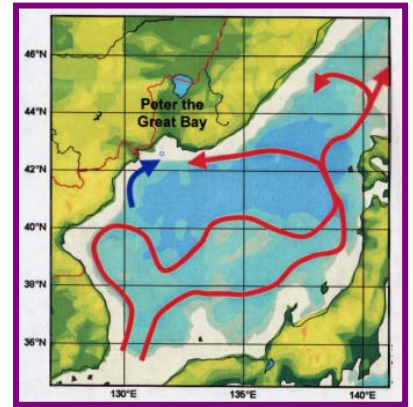
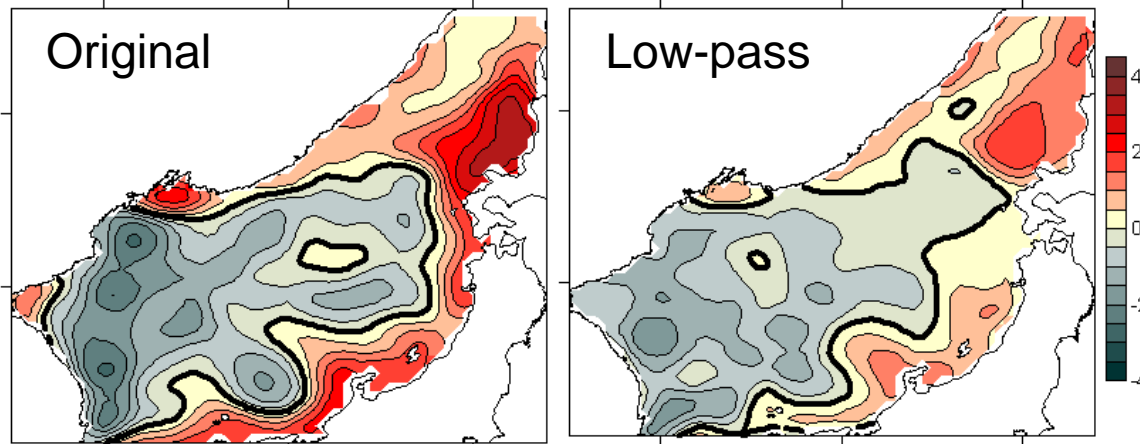


QB variations in the atmospheric ‘centers of actions’, such as North Pacific High (Angell et al., 1969).

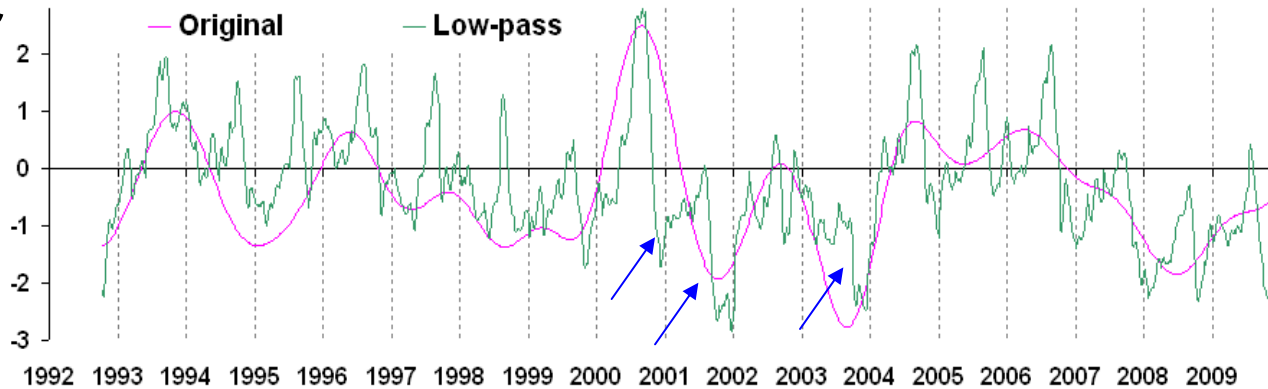


Seasonal and interannual Pathway Mode

EOF



PC

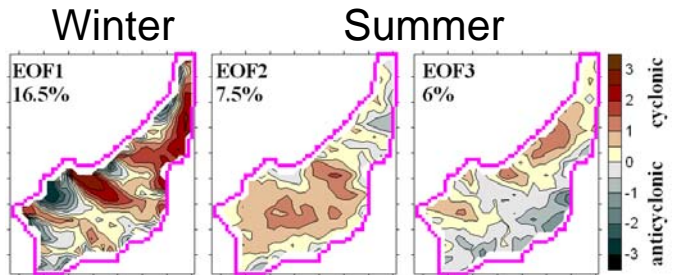


Seesaw between the western/central JES and eastern JES – between two major pathways of the northward transport of water

Seasonal signal (improvement from $1/3^\circ$ -gridded SLA): the negative phase from fall through late winter or spring, weakening in late winter, while the positive phase is in late summer.

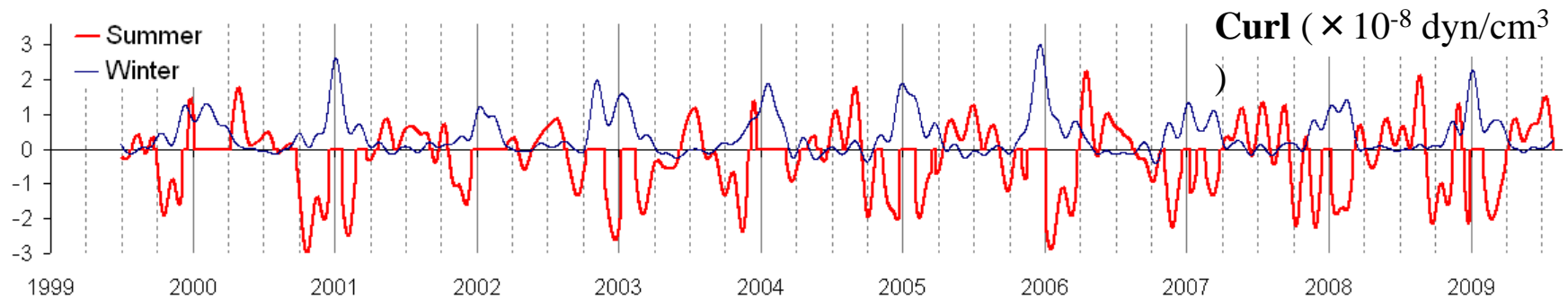
Seasonal wind stress curl

EOF decomposition of stress curl from QSCAT winds (this afternoon)

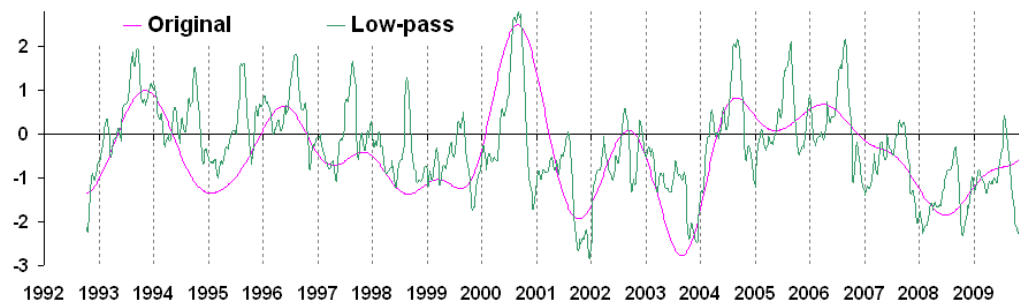
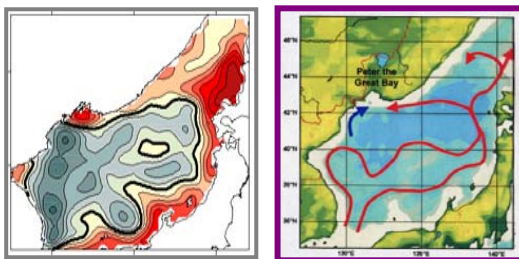


Curl low-pass filtered with the cut-off period of 40 days.

AC curl in late winter/spring and fall;
cyclonic to zero oscillating curl in late summer
(confirmation of the previous qualitative considerations
from NCEP winds; Trusenkova et al., 2006-2009).

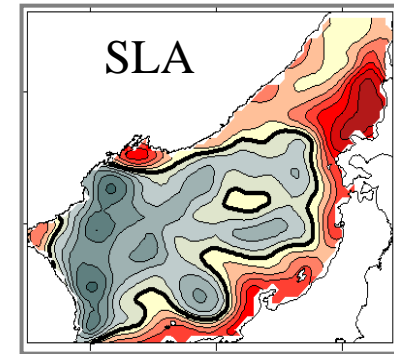


Blue curve is for the contribution from the winter mode and red curve from two summer modes.

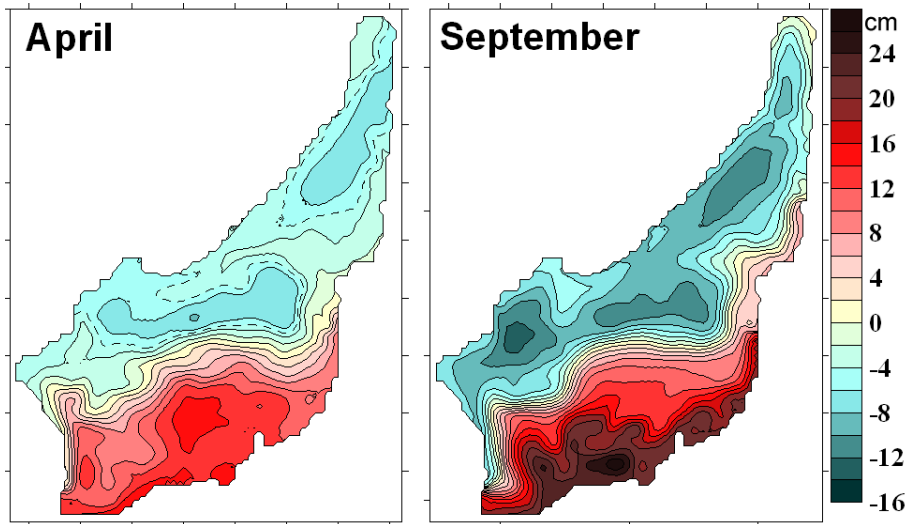


Forcing by wind stress curl

Well known NW branch of SAF in fall (Yoon et al., 2005; Yoon and Kim, 2009; Trusenkova et al., 2005, 2009).



Numerical simulation with an oceanic model



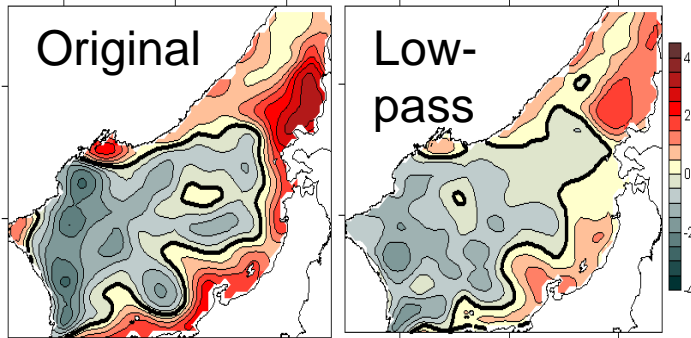
NW branch of SAF in spring, as well as in fall documented from infrared satellite imagery (Nikitin, 2006).

Negative phase (the intensified AC circulation in the western JES) forced by the AC wind curl in fall and late winter/spring – 'anticyclonicity'.

Positive phase (the intensified TWC and its westward branch) forced by the C curl in late summer – 'cyclonicity'.

SSH pattern for September corresponds to the summer circulation scheme by Yoon and Kim (2009).

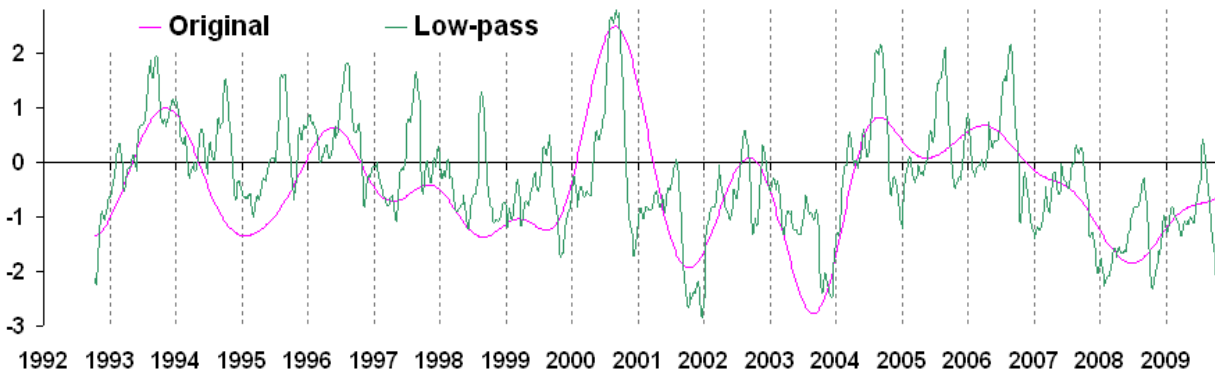
Interannual Pathway Mode



Periods of *QB* variability (1993-1996, 2000-2004).

QB variability in the southern JES
(path variations of the TWC)
(Hirose and Ostrovskii, 2000; Choi et al., 2004).

Extreme event: The strongest positive phase in summer 2000 and the absent EKWC from June to October 2000 (Chang et al., 2004).



Different regimes:

Positive phase
(‘cyclonicity’):
1993, 1996, 2000, 2004-
2006.

Negative phase
(‘anticyclonicity’):
1997-1999, 2001-2003,
2007-2009.

Forcing of the Interannual Pathway not evident – interannual wind variability?

Conclusion

- The same seasonal signals from the reference and update AVISO SLA, while the interannual SLA differ.
- No secular trends.
- Quasi-biennial synchronous oscillation.
- No interannual change of the circulation strength in terms of statistical patterns.
- The seasonal Pathway Mode from the $1/4^\circ$ -gridded AVISO product is improved. It can be explained by the circulation changes forced by wind stress curl.
- Interannual circulation regimes of the strengthened cyclonicity vs. anticyclonicity.

